

Antibacterial Activity and Mechanism of Candesartan Cilexetil against *Enterococcus faecalis*

Chengchun Chen,⁺ Duoyun Li,⁺ Yongpeng Shang,⁺ Zhiwei Lin,⁺ Zewen Wen, Peiyu Li, Zhijian Yu, Zhong Chen,^{*} and Xiaoju Liu^{*}



Cite This: *ACS Omega* 2024, 9, 21510–21519



Read Online

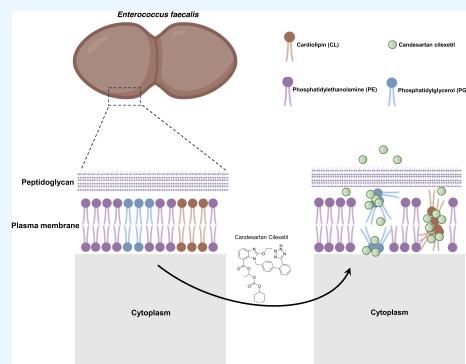
ACCESS |

Metrics & More

Article Recommendations

Supporting Information

ABSTRACT: *Enterococcus faecalis* infections pose a significant clinical challenge due to their multidrug resistance and propensity for biofilm formation. Exploring alternative treatment options, such as repurposing existing drugs, is crucial in addressing this issue. This study investigates the antibacterial activity of candesartan cilexetil against *E. faecalis* and elucidates its mechanism of action. Candesartan cilexetil exhibited notable antibacterial activity against both *E. faecalis* and *Enterococcus faecium*, with minimum inhibitory concentration (MIC) of $\leq 25 \mu\text{M}$. Time-kill curves demonstrated concentration-dependent bactericidal effects. Candesartan cilexetil could significantly inhibited biofilm formation at the concentration of $1/4\times$ MIC and induced alterations in biofilm structure. Permeability assays revealed compromised bacterial membranes, accompanied by the dissipation of membrane potential in *E. faecalis* cells after treatment with candesartan cilexetil. Checkerboard analysis showed that bacterial membrane phospholipids phosphatidylglycerol and cardiolipin could neutralize the antibacterial activity of candesartan cilexetil in a dose-dependent manner. Bilayer interferometry (BLI) assay indicated specific interactions between candesartan cilexetil and phosphatidylglycerol or cardiolipin. This study demonstrates the promising antibacterial and antibiofilm activities of candesartan cilexetil against multidrug-resistant *E. faecalis*. The mechanism of action involves disruption of bacterial membranes, possibly by interacting with membrane phospholipids. These findings underscore the potential utility of candesartan cilexetil as an effective therapeutic agent for combating *E. faecalis* infections, offering a valuable strategy in the battle against antibiotic-resistant pathogens.



INTRODUCTION

Enterococcus faecalis, a clinically significant Gram-positive pathogen, is associated with various infectious diseases, including bacteremia, intra-abdominal infections, endocarditis, and urinary tract infections.¹ The ability of *E. faecalis* to tolerate oxidative stress, desiccation, extreme temperatures, pH variations, as well as its intrinsic resistance to salt, bile acids, and detergents, has allowed it to adapt and survive in diverse adverse environments, including hospital settings and non-living surfaces.² Consequently, it has emerged as a major nosocomial pathogen responsible for hospital-acquired infections.³ One of the challenges in the clinical management of *E. faecalis* infections is its intrinsic multidrug resistance, as most clinical isolates exhibit resistance to cephalosporins, aminoglycosides, lincosamides, and streptogramin antibiotics.⁴ Furthermore, the presence of mobile genetic elements such as plasmids and transposons has accelerated the transfer and dissemination of resistance genes in *E. faecalis*.^{5–8} In recent years, the problem of antibiotic resistance in *E. faecalis* infections has become increasingly severe, particularly with the rise of resistance to first-line antimicrobial drugs such as vancomycin, daptomycin, and linezolid, leading to limited

treatment options in the clinical setting.^{9–12} As a consequence, there is an urgent need for the development of novel antibacterial agents targeting *E. faecalis*.

Another significant factor contributing to the failure of clinical treatment in *E. faecalis* infections is the formation of biofilms. Over 40% of clinical isolates of *E. faecalis* are capable of forming biofilms,¹³ and previous studies from our research group have highlighted biofilm formation as a major challenge in *E. faecalis* treatment.^{14–16} Biofilms represent structured communities of microorganisms, where bacteria adhere to surfaces and are encased within a self-produced extracellular polymeric matrix. The presence of biofilms in *E. faecalis* infections not only impedes eradication efforts but also serves as a focus for bacterial dissemination and a reservoir for antibiotic resistance genes.¹⁷ *E. faecalis* biofilms have been

Received: March 5, 2024

Revised: April 8, 2024

Accepted: April 12, 2024

Published: May 3, 2024



implicated in various infections, including those in the urinary tract, wounds, diseased gastrointestinal tract, and endocarditis. Biofilm formation confers increased resistance to antibiotics, host immune responses, and various stressors, promoting the persistence of bacterial infections, posing significant challenges to clinical antimicrobial therapy.^{18,19} Notably, clinical *E. faecalis* biofilm formation has been positively correlated with antibiotic resistance, with mature biofilms demonstrating resistance to antibiotics at concentrations 10 to 1000 times higher than those needed to kill planktonic bacteria.²⁰ Therefore, there is a pressing need to explore novel antibacterial agents that can effectively inhibit both planktonic growth and biofilm formation or eradicate established biofilms, in order to enhance the clinical practice efficacy against multidrug-resistant *E. faecalis* infections.

In recent years, drug repurposing has emerged as a promising strategy in the discovery of new antibacterial agents. This approach involves the exploration of existing drugs for their hidden antibacterial activities. Given the escalating threat of antibiotic resistance, the options for treating multidrug resistant bacteria are becoming increasingly limited. Furthermore, the pharmaceutical industry has reduced its focus on antibacterial drug research, redirecting investments toward therapeutic areas with higher returns on investment.²¹ Therefore, drug repurposing as a strategic approach in antibacterial drug research is gaining attention, offering the potential to reduce costs and expedite approval timelines.²² In light of the growing concerns over antibiotic resistance and biofilm-related challenges in *E. faecalis* infections, we screen the potential of FDA-approved clinical drugs to combat this clinically important pathogen. It was then found that candesartan cilexetil showed superior antibacterial activity against both standard and clinical strains of *E. faecalis*. Candesarant cilexetil is an angiotensin II receptor blocker widely used for the treatment of hypertension and heart failure. It exerts its therapeutic effects by selectively blocking the action of angiotensin II, a hormone that constricts blood vessels and raises blood pressure. Due to its efficacy and safety profile, candesartan cilexetil has become a popular choice in clinical practice. Here, we evaluated the antimicrobial and antibiofilm activity of candesartan cilexetil against *E. faecalis*, and the mechanism of antibacterial action was also studied. Our study aiming to shed light on the development of promising therapeutic approaches to address the increasing threat posed by multidrug-resistant *E. faecalis* infections.

RESULTS

Candesartan Cilexetil Exhibits Antibacterial Activity against *E. faecalis*. In the pursuit of identifying potential antibacterial compounds against *E. faecalis*, we conducted a screening of chemicals using the FDA-Approved Drugs Library. Remarkably, we discovered that candesartan cilexetil exhibited inhibitory activity against the *E. faecalis*. The MIC of candesartan cilexetil for standard strains *E. faecalis* ATCC 29212 and *Enterococcus faecium* ATCC 35667 was both 25 μM . To further investigate its antibacterial potential, we determined the MIC of candesartan cilexetil against 40 clinical *E. faecalis* isolates, which including 10 linezolid-resistant *E. faecalis*. The results demonstrated that candesartan cilexetil displayed MIC values ranging from 12.5 μM ($\approx 7.63 \mu\text{g/mL}$) to 25 μM ($\approx 15.27 \mu\text{g/mL}$) against clinical *E. faecalis* isolates (Table 1). Importantly, it is worth noting that candesartan cilexetil exhibited comparable antimicrobial activity against linezolid-

Table 1. Antimicrobial Activity of Candesarant Cilexetil against *E. faecalis* and *E. faecium*

strain	no.	MIC distribution (μM) ^a			
		6.25	12.5	25	MIC ₅₀ ^b /MIC ₉₀ ^c
<i>E. faecalis</i>	30	1	2	27	25/25
LRE	10	0	2	8	25/25
<i>E. faecium</i>	10	0	3	7	25/25

^aMIC, minimal inhibitory concentration, was determined as the lowest concentration of candesartan cilexetil that showed no visible growth in the plate. ^bMIC₅₀ refers to the concentration that would inhibit the growth of 50% of the tested bacterial isolates. ^cMIC₉₀ refers to the concentration that would inhibit the growth of 90% of the tested bacterial isolates.

resistant *E. faecalis* (LRE) isolates, with both MIC₅₀ and MIC₉₀ values measured at 25 μM . The minimum bactericidal concentrations (MBCs) of clinical *E. faecalis* isolates toward candesartan cilexetil ranged from 25 to 100 μM (Table S1). To understand its inhibitory effects on bacterial growth, we conducted growth curve experiments. The data revealed that candesartan cilexetil effectively inhibited the growth of planktonic cells of *E. faecalis* in a dose-dependent manner, with concentrations ranging from 1/8 \times to 1 \times MIC (Figure 1A,B). Furthermore, candesartan cilexetil exhibited robust antibacterial activity against *E. faecium*, with a MIC of $\leq 25 \mu\text{M}$. These findings highlight candesartan cilexetil's broad-spectrum antimicrobial potential, encompassing not only *E. faecalis* but also *E. faecium*, another clinically significant pathogen known for its association with healthcare-associated infections and antibiotic resistance. The development of resistance against *E. faecalis* was assessed by serially passaging 16C166 in various concentrations of candesartan cilexetil for 60 days, corresponding to 30 passages. The antibacterial activity of the positive control antibiotic, linezolid, exhibited a rapid decline after approximately 10 passages. In contrast, candesartan cilexetil maintained its effectiveness throughout the experiment (Figure 1C). These findings indicated that *E. faecalis* have difficulty developing resistance to candesartan cilexetil.

Time-Killing Curves of Candesarant Cilexetil against *E. faecalis*. The results of the time-kill experiments that investigated the clinical isolate *E. faecalis* EF16C166 are presented in Figure 2 and visually depict the bactericidal activity of candesartan cilexetil against *E. faecalis*. As seen in Figure 2A, candesartan cilexetil at 1 \times MIC and 2 \times MIC showed weak bactericidal activity for *E. faecalis* EF16C166, whereas daptomycin at 8 \times MIC showed a weaker activity. Moreover, when a candesartan cilexetil concentration up to 4 \times MIC, in the first 6 h, no bacterial colony was counted on the plate after incubated at 37 $^{\circ}\text{C}$ for 24 h. When the concentration of candesartan cilexetil reached 8 \times MIC, the remaining CFU at 2 h reached the lower limit of detection, which demonstrated that candesartan cilexetil had excellent bactericidal effect. Furthermore, candesartan cilexetil was evaluated for its synergistic effect in combination with daptomycin against *E. faecalis* using a checkerboard test. As shown in Table 2, the fractional inhibitory concentration index (FICI) of candesartan cilexetil in combination with daptomycin was < 0.5 , indicating a synergistic effect. In addition, candesartan cilexetil combined with daptomycin exhibited synergistic bactericidal activity against *E. faecalis*, and low concentration (1/2 \times MIC) of candesartan cilexetil could

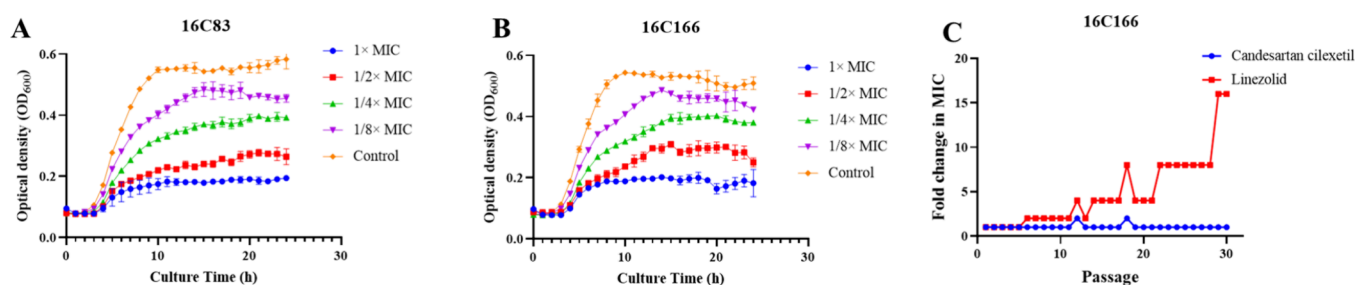


Figure 1. Impact of candesartan cilexetil on *E. faecalis*. (A, B) Effect of varying concentrations of candesartan cilexetil on growth curves of clinical *E. faecalis* isolates. The isolates utilized in the experiment exhibited a MIC of 25 μ M, with candesartan cilexetil concentrations (1/8 \times , 1/4 \times , 1/2 \times , and 1 \times MIC) subjected to testing. Optical density at a wavelength of 600 nm (OD_{600}) was measured at hourly intervals over a 24-h period. The presented data are depicted as means \pm standard deviation (SD). (C) Development of resistance after 60 days of serial passaging using sub-MIC of candesartan cilexetil and the positive control, linezolid, against *E. faecalis* 16C166.

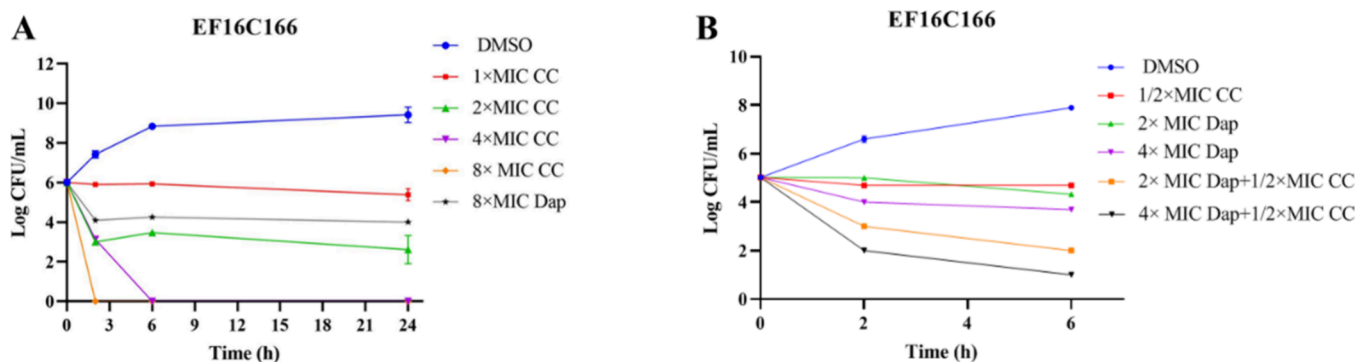


Figure 2. Analysis of the bactericidal activity of candesartan cilexetil against *E. faecalis* planktonic cells. (A) *E. faecalis* 16C166 in exponential growth phase was challenged with candesartan cilexetil at 4 \times MIC. Bacteria were counted on TSB agar plates at 0, 2, 6, and 24 h after challenge. (B) Bactericidal activity of 1/2 \times MIC candesartan cilexetil in combination with daptomycin against *E. faecalis* planktonic cells. CC, candesartan cilexetil; dap, daptomycin.

Table 2. FICI Results of the Combination of Daptomycin and Candesartan Cilexetil against *E. faecalis*

isolates	MIC (μ g/mL)		in combination	FICI ^b	synergy ^c
	daptomycin (μ g/mL)	CC (μ M) ^a			
ATCC29212	2	25	0.25/6.25	0.375	+
16C51	2	25	0.5/1.56	0.3125	+
16C83	2	25	0.25/3.13	0.25	+
16C166	1	25	0.125/6.25	0.375	+

^aCC, candesartan cilexetil. ^bFICI, fractional inhibitory concentration index. ^cThe FICI results were interpreted as follows: FICI \leq 0.5 = synergy; FICI > 4.0 = antagonism; and FICI > 0.5–4 = indifference.²³

significantly enhance the bactericidal activity of daptomycin against *E. faecalis* (Figure 2B).

Candesartan Cilexetil Showed an Effective Antibiofilm Activity against *E. faecalis*. Candesartan cilexetil was assessed at sub-MICs to determine its ability to prevent the formation of biofilms produced by *E. faecalis*. To quantify the biomass of the biofilms, a crystal violet (CV) staining method was employed. As depicted in Figure 3A, the introduction of 1/4 \times MIC of candesartan cilexetil effectively hindered the biofilm formation across all tested strains. Complementary to the outcomes from crystal violet staining, the utilization of CLSM provided visual insights into the impact of candesartan cilexetil on *E. faecalis* biofilms. Corresponding with the results of crystal violet staining, discernible inhibition of biofilm formation due to 1/4 \times MIC of candesartan cilexetil was evident in the CLSM images (Figure 3B). The effect of candesartan cilexetil on *E. faecalis* in the mature biofilm was further evaluated using the minimal biofilm inhibitory (MBIC)

and minimal eradication concentrations (MBEC) assay. The MBIC and MBEC values determined are listed in Table S2. In general, the MBIC values were 2–8 times higher compared to the MIC, whereas the MBEC values were 4–16 times higher compared to the MIC. Consistent with that, 4 \times MIC candesartan cilexetil challenge resulted in a >3 log decrease in CFU compared to the untreated control (Figure 3C). These collective results underscore the substantial antibiofilm activity of candesartan cilexetil against *E. faecalis*.

Proteomic Analysis of *E. faecalis* Treated with Candesartan Cilexetil. We conducted a proteomic analysis to delve into the antimicrobial mechanism of candesartan cilexetil. Utilizing mass spectrometry, we scrutinized the proteomic response of *E. faecalis* treated with candesartan cilexetil at 1/2 \times MIC and compared it to treatment with DMSO alone. Impressively, a total of 1265 proteins were confidently identified, meeting the criteria of having matched peptides \geq 1 and a false discovery rate (FDR) < 0.01. Notably,

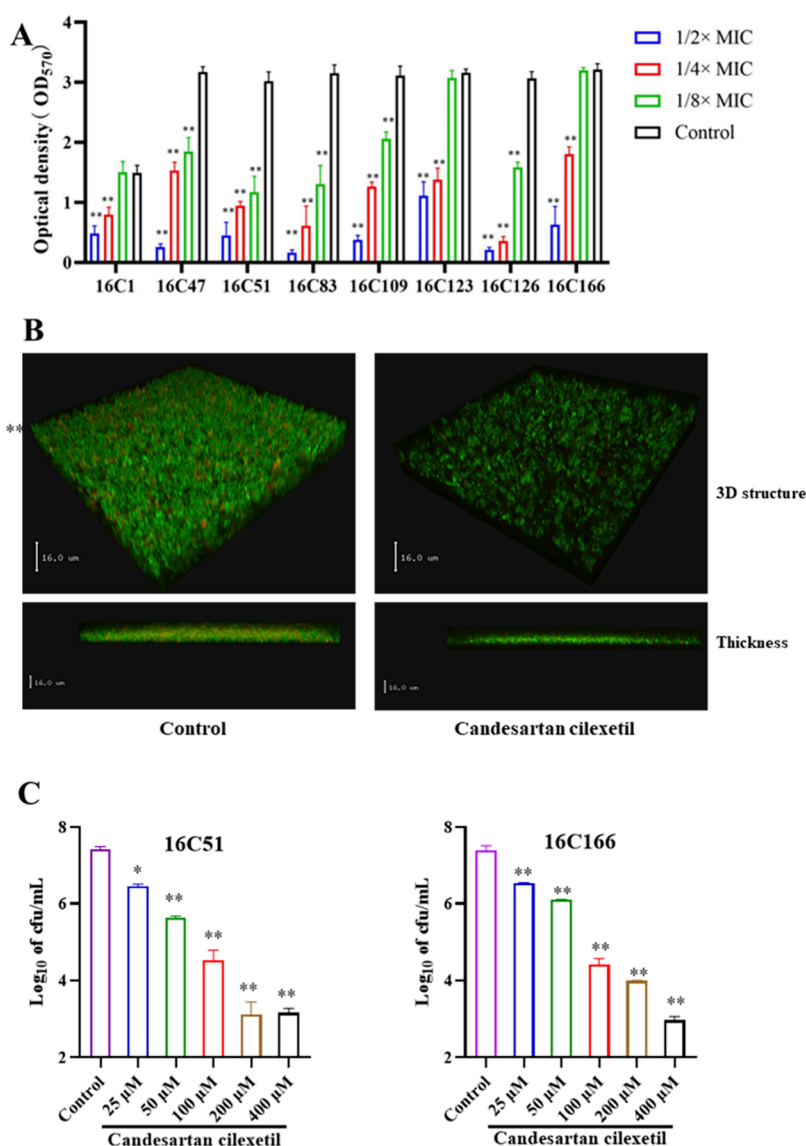


Figure 3. Antibiofilm activity of candesartan cilexetil against *E. faecalis*. (A) Eight clinical *E. faecalis* isolates were tested for the inhibitory effect of candesartan cilexetil on the biofilm formation under subinhibitory concentrations. (B) Effect of candesartan cilexetil on the biofilm formation of the *E. faecalis* observed by CLSM. A subminimal inhibitory concentration (sub-MIC) of 1/4× MIC (6.25 μM) candesartan cilexetil was introduced to cultures of *E. faecalis*. After 24 h of incubation, the biofilms that developed on a glass coverslip within a cell culture dish were subjected to live/dead viability staining and subsequently visualized using CLSM technology. (C) The reduction in CFU count of *E. faecalis* cells in biofilms at various concentrations of candesartan cilexetil was compared to the corresponding untreated biofilms. Data are represented as means ± SD **P* < 0.05; ***P* < 0.01 (two-tailed Student's *t* test).

144 proteins exhibited significant variations in expression levels (≥ 1.5 -fold change, $P \leq 0.05$) when contrasted with the control group. This subset comprised 40 upregulated and 104 downregulated proteins following candesartan cilexetil treatment (Figure 4A). Employing gene ontology (GO) annotations based on biological processes, we found that the differentially expressed proteins were prominently enriched in processes related to stress response, protein folding, and the negative regulation of transcription, DNA-templated (Figure 4B). To further comprehend the protein–protein interactions (PPI), we constructed a network analysis using the STRING database. The findings unveiled that the down-regulated proteins were mainly concentrated in ATP synthase Phenylalanine, tyrosine and tryptophan biosynthesis, which means that candesartan cilexetil treatment resulted in impaired energy metabolism in *E. faecalis* (Figure 4C). The upregulated

proteins were associated with enzymes connected to ABC transporters, heat shock proteins, and the protease system. This list included proteins like *grpE*, *groEL*, *HrcA*, *clpB*, *clpP*, and *dnaK*. This observation pointed toward candesartan cilexetil's potential to disrupt the protein homeostasis of *E. faecalis*. These proteins constitute crucial stress responders pivotal in maintaining cellular equilibrium. Additionally, the ABC transporters exhibited a role in potentially reducing the concentration of drugs within bacterial cells (Figure 4D).

Candesartan Cilexetil Caused Damage to the Cell Membrane System of *E. faecalis*. In order to explore whether the strong bactericidal effect of candesartan cilexetil on *E. faecalis* is related to damage to the cell membrane system, we employed propidium iodide (PI) fluorescent dye to evaluate the impact of candesartan cilexetil on cytoplasmic membrane permeability and fluorescent dye DiBAC4(3) to

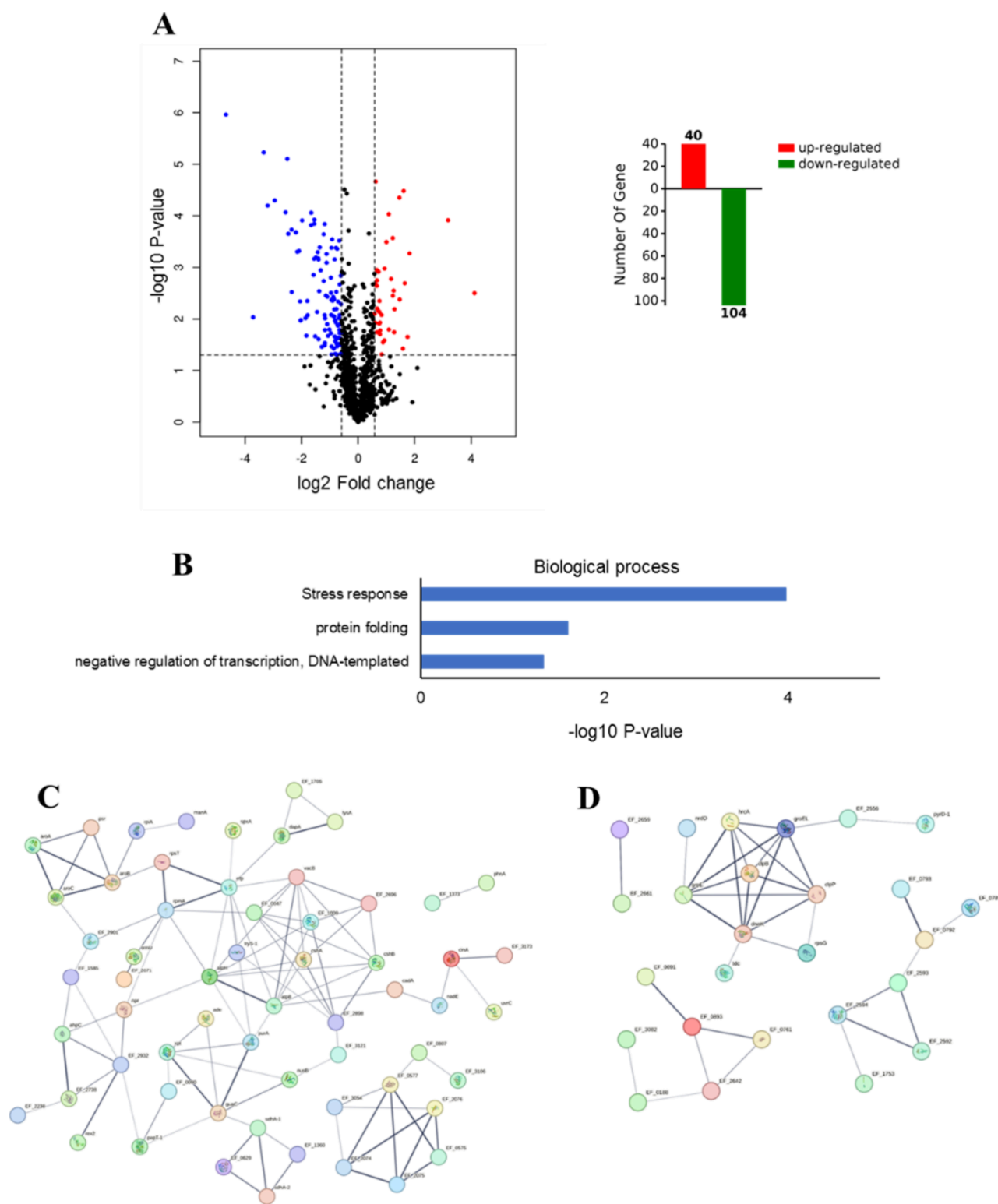


Figure 4. Differential expression analysis of proteins upon treatment with candesartan cilexetil. (A) Volcano plot depicting the differential expression of proteins between *E. faecalis* groups treated with candesartan cilexetil and untreated groups. Red points indicate upregulated proteins, while blue points represent downregulated proteins. (B) Gene Ontology (GO) analysis conducted on differentially expressed proteins, categorized according to biological processes. (C, D) Protein–protein Interaction (PPI) network analysis for downregulated proteins upon candesartan cilexetil treatment based on the STRING database. The thickness of the connecting lines signifies the strength of data.

assess its effect on membrane potential. When treating cells of *E. faecalis* 16C166 with PI, the introduction of candesartan cilexetil from $1\times$ MIC to $4\times$ MIC resulted in a marked increase in fluorescence intensity, with a positively correlated

rise corresponding to the concentration (Figure 5A). Conversely, in the case of OG1RF cells treated with DiBAC4(3) dye, candesartan cilexetil induced a rapid escalation in fluorescence intensity in a dose-dependent

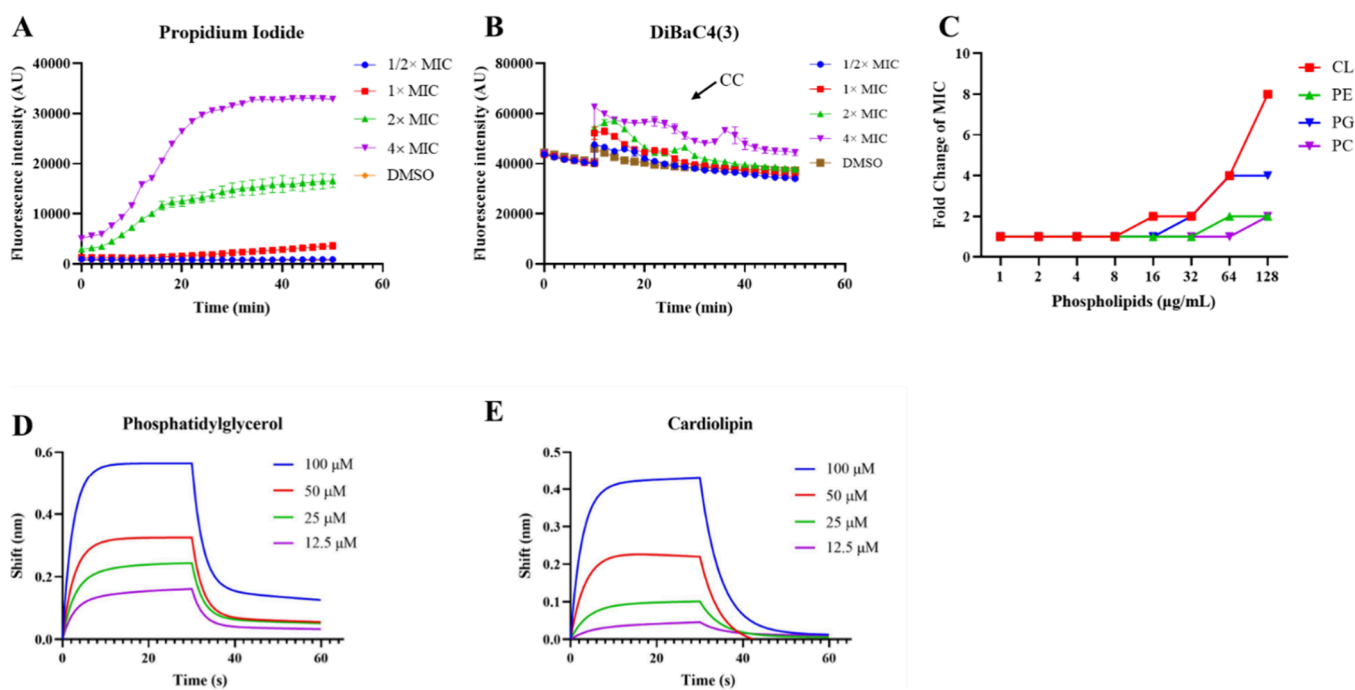


Figure 5. Impact of candesartan cilexetil on the cytoplasmic membrane of *E. faecalis*. The *E. faecalis* 16C166 cells were treated with various concentrations of candesartan cilexetil, and the membrane permeability (A) and membrane potential (B) were monitored by fluorescent dye propidium iodide and DiBaC4(3), respectively. (C) The antibacterial activities of candesartan cilexetil supplied with exogenous addition of phosphatidylglycerol (PG), phosphatidylethanolamine (PE), phosphatidylcholine (PC), and cardiolipin (CL) against *E. faecalis* 16C166 were determined by checkerboard microdilution method. (D, E) Kinetic analysis by BLI of the binding of candesartan cilexetil to phosphatidylglycerol and cardiolipin.

manner from 1/2× MIC to 4× MIC (Figure 5B), indicating that the cells experienced depolarization. Furthermore, we analyzed which components of the cell membrane candesartan cilexetil acts on. Checkerboard analysis showed that membrane phospholipids phosphatidylglycerol (PG) and cardiolipin (CL) could neutralize the antibacterial activity of candesartan cilexetil in a dose-dependent manner (Figure 5C). phosphatidylcholine (PC), which was not detected in *E. faecalis* but enriched in mammalian cell membranes,^{24,25} only had a negligible inhibitory effect on the activity of candesartan cilexetil. Finally, we used BLI to further demonstrate that candesartan cilexetil can directly interact with PG and CL (Figure 5D,E). BLI kinetic analysis showed that the KD values of candesartan cilexetil with PG and CL were 73.5 μM and 62.9 μM , respectively. Taken together, candesartan cilexetil may disrupt cell membrane integrity by targeting membrane phospholipids PG and CL.

DISCUSSION

The emergence of multidrug-resistant *E. faecalis* isolates has posed a significant challenge in the clinical management of infections caused by this pathogen. In this study, we investigated the antibacterial potential of candesartan cilexetil, an FDA-approved drug commonly used for hypertension and heart failure treatment, against *E. faecalis*. The results demonstrated that candesartan cilexetil exhibited remarkable antibacterial activity against both standard and clinical strains of *E. faecalis*, including linezolid-resistant isolates. This finding is of paramount importance considering the increasing prevalence of antibiotic-resistant strains and the limited therapeutic options available. Furthermore, the antimicrobial effect of candesartan cilexetil was not confined to *E. faecalis*

alone, as it also displayed substantial activity against *E. faecium*, another clinically relevant pathogen associated with antibiotic resistance and nosocomial infections.²⁶ Our study provides valuable insights into the antibacterial potential of candesartan cilexetil against *E. faecalis*. The demonstrated activity against both planktonic cells and biofilm formations, highlights candesartan cilexetil as a promising candidate for further development as an antibacterial agent. Considering the growing concerns surrounding antibiotic resistance and the urgent need for novel therapeutic approaches, the repurposing of candesartan cilexetil could offer a viable strategy for combating multidrug-resistant *E. faecalis* infections. Further investigations, including *in vivo* studies and clinical trials, are warranted to validate the potential clinical utility of candesartan cilexetil as an antibacterial agent against *E. faecalis* infections and to explore its broader applicability against other bacterial pathogens.

Biofilm formation is a critical survival strategy employed by many bacterial species, including *E. faecalis*, to thrive in various environments and evade host immune responses.¹⁷ Biofilms are intricate communities of bacteria embedded within a self-produced extracellular matrix, comprising proteins, polysaccharides, and nucleic acids.¹⁷ This protective matrix provides structural integrity and shields bacteria from antimicrobial agents and host defenses, making biofilm-associated infections extremely challenging to treat. In the context of *E. faecalis* infections, biofilm formation is not only implicated in persistent infections but also in the dissemination of antibiotic resistance genes within the bacterial population.^{27,28} Our study unveiled the promising antibiofilm activity of candesartan cilexetil against *E. faecalis*. The ability of candesartan cilexetil to inhibit biofilm formation and disrupt mature biofilms suggests

its potential to mitigate the challenges posed by biofilm-related infections. Candesartan cilexetil's dual action against planktonic cells and biofilms reflects a holistic approach to combating infections caused by *E. faecalis*.

To unravel the mechanism underlying the antibacterial action of candesartan cilexetil, we employed proteomic analysis. The results revealed significant alterations in the expression levels of proteins associated with stress response, protein folding, and transcriptional regulation. Notably, upregulated proteins were enriched in ABC transporters, heat shock proteins, and the protease system. These findings suggest that candesartan cilexetil might disrupt protein homeostasis in *E. faecalis*, thereby perturbing cellular stress response mechanisms and potentially enhancing susceptibility to antibacterial agents. Moreover, the observed downregulation of proteins related to energy metabolism highlights the potential of candesartan cilexetil to interfere with bacterial metabolic processes. The disruption of energy metabolism in *E. faecalis* due to downregulated proteins highlights the multifaceted impact of candesartan cilexetil on bacterial physiology.

One of the notable mechanisms through which candesartan cilexetil exerts its antibacterial activity is by affecting the cell membrane system of *E. faecalis*. The increase in membrane permeability and the loss of membrane potential observed upon treatment with candesartan cilexetil suggest that it may induce damage to the bacterial cell membrane. Furthermore, our studies on the interactions between candesartan cilexetil and membrane phospholipids, such as phosphatidylglycerol and cardiolipin, indicate a direct binding affinity. This provides valuable insights into the molecular basis of candesartan cilexetil's action on the cell membrane and its potential role in disrupting membrane integrity.

CONCLUSIONS

In summary, our study sheds light on the potential of candesartan cilexetil as an effective antibacterial agent against *E. faecalis*. Its antimicrobial and antibiofilm activities, coupled with its mechanism of action involving disruption of protein homeostasis and cell membrane integrity, highlight its promising potential as a therapeutic candidate for the treatment of multidrug-resistant infections. The drug repurposing approach employed in this study underscores the significance of exploring existing drugs for hidden antibacterial activities, offering a cost-effective and efficient strategy for addressing the challenges posed by antibiotic-resistant pathogens.²⁹ Overall, the findings of this study highlight the potential of candesartan cilexetil as a novel antibacterial agent against *E. faecalis*. Its antibacterial properties, combined with its established safety profile as an antihypertensive drug, make it a promising candidate for further development as a therapeutic option for infectious diseases caused by *E. faecalis*.

METHODS

Strains and Cultural Conditions. The clinical strains of *E. faecalis*, and *E. faecium* used in this study were collected from different hospitalized patients at Huazhong University of Science and Technology Union Shenzhen Hospital between 2015 and 2018. All clinical isolates were initially identified using the Phoenix 100 automated microbial identification system, and after subculture, all strains were reidentified using matrix-assisted laser desorption/ionization time-of-flight mass

spectrometry (MALDI-TOF-MS). Quality control strains of *E. faecalis* ATCC29212 and *E. faecium* ATCC35667 were obtained from the ATCC strain repository.

Determination of Minimal Inhibitory Concentrations.

The minimal inhibitory concentrations (MICs) of candesartan cilexetil and linezolid were determined using the broth microdilution method, following the guidelines provided by the Clinical and Laboratory Standards Institute (CLSI). Briefly, overnight cultures of each strain were diluted in cation-adjusted Mueller Hinton broth (CAMHB) to achieve a final concentration of approximately 5×10^5 CFU/mL. Subsequently, the bacterial suspensions were incubated in a 96-well plate with a gradient of compound concentrations at 37 °C for 18 h. The MIC was determined as the lowest concentration of antibiotics that showed no visible growth in the plate. *E. faecalis* ATCC29212 and *E. faecium* ATCC35667 were utilized as quality controls.

Time-Kill Assay. Mid log-phase cells of *E. faecalis* isolates were adjusted to a 0.5 McFarland standard and then further diluted 1:100 with Tryptic Soy Broth (TSB). Subsequently, the bacterial suspensions were treated with different concentrations of candesartan cilexetil and incubated at 37 °C with continuous shaking at 220 rpm. Samples were collected at time points of 0, 3, 6, and 24 h, followed by washing and serial dilution in sterile normal saline. The diluted samples were then plated on Tryptic Soy Broth (TSB) agar plates for bacterial colony counting after incubating for 24 h at 37 °C.

Biofilm Inhibition Assay. Overnight cultures of *E. faecalis* isolates were diluted 1:200 in TSB medium supplemented with 2% glucose. The diluted cultures were then added to a 96-well flat-bottom plate, with varying concentrations of candesartan cilexetil or an equal volume of dimethyl sulfoxide (DMSO) for the control group. The plate was incubated statically at 37 °C for 24 h. After incubation, the medium was discarded, and the biofilms were washed twice with phosphate-buffered saline (PBS) to remove any planktonic cells. To quantify the biofilm biomass, each well was stained with 0.1% crystal violet and the optical density at 570 nm was measured.

Microscopic Observation of Biofilm Morphology. The efficiency of candesartan cilexetil in *E. faecalis* cells embedded in the biofilm was visually assessed by a confocal laser scanning microscope (CLSM). The overnight culture of *E. faecalis* 16C166 was 1:200 diluted with fresh TSBG medium and placed into the cell-culture dish (Corning, United States) and cultured at 37 °C for 24 h to form mature biofilms. To prepare the samples for confocal microscopy, the biofilms were washed with PBS and then stained with 1 μ M SYTO9 and 1 μ M propidium iodide (PI) for 15 min in the dark. The stained biofilms were visualized using a Confocal Laser Scanning Microscope (CLSM, Olympus Corporation) to examine the biofilm morphology.

Antibacterial Activity of Candesartan Cilexetil with Phospholipids. Various phospholipids, such as phosphatidylglycerol (PG, Aladdin, China), Phosphatidylethanolamine (Y0001953, Sigma-Aldrich, USA), or cardiolipin (CL, Sigma-Aldrich, C0563, USA), were dissolved in methanol. The impact of phospholipids (ranging from 1 to 128 μ g/mL) on the MIC values of candesartan cilexetil in CAMHB medium was assessed using the checkerboard method as described.²³

Membrane Permeability Assay. Mid log-phase cells of OG1RF were washed three times with sterile PBS and adjusted to a 0.5 McFarland turbidity. The cell suspension was then further diluted 1:10. Subsequently, the cells were incubated

with 2 μM PI at 37 $^{\circ}\text{C}$ for 10 min. Afterward, the cell suspension was treated with different concentrations of candesartan cilexetil 0.1% Triton X-100, or 0.1% DMSO. The treated cell suspensions were incubated in a 96-well plate with a black border and transparent bottom. The fluorescence intensity was dynamically monitored at an excitation wavelength of 493 nm with an emission wavelength of 534 nm. This assay allowed for the assessment of changes in cell membrane integrity based on the fluorescence intensity of PI-stained cells in response to different treatments.

Membrane Potential Determination. Mid log-phase cells of OG1RF were washed three times with PBS, then adjusted to a 0.5 McFarland turbidity, and further diluted 1:10. Subsequently, the cells were incubated with 1 μM DiBaC4(3) at 37 $^{\circ}\text{C}$ for 10 min. After the incubation, the cell suspension was treated with different concentrations of candesartan cilexetil (12.5–100 μM) or 0.1% DMSO as a control. The treated cell suspensions were then incubated in a 96-well plate with a black border and transparent bottom. The fluorescence intensity was dynamically monitored at an excitation wavelength of 492 nm with an emission wavelength of 515 nm. This assay enabled the evaluation of changes in cell membrane potential based on the fluorescence intensity of DiBaC4(3)-stained cells in response to different treatments.

Resistance Development Assay. *E. faecalis* 16C166 overnight cultures were diluted 1:100 into MH broth containing 1/2 \times MIC of candesartan cilexetil or linezolid. The bacterial culture was diluted 1:100 and transferred to a fresh medicated medium after 48 h of incubation at 37 $^{\circ}\text{C}$ to start the subsequent generation. MIC values were determined after every passages. The serial passage was continued for 60 days, corresponding to 30 passages.

Determination of MBIC and MBEC. MBICs and MBECs were determined using a Calgary biofilm device (catalog No. 445497, Nunc, Denmark).³⁰ Bacterial suspension from overnight culture was inoculated to 150 μL TSBG in the wells of a microtiter plate followed by the application of a lid with 96 pegs. Biofilm was allowed to form on the lid pegs of the lid by incubation for 24 h and 100 rpm. The peg lids were then transferred to place into new 96-well plates containing 2-fold dilutions of TSBG with candesartan cilexetil and were incubated for an additional 24 h and 100 rpm. After candesartan cilexetil challenge, the pegs were rinsed twice with sterile PBS and placed into a new 96-well plate containing 150 μL of recovery medium. The biofilm cells were dislodged from the pegs to recovery medium by sonication for 20 min. The recovery medium was incubated for 18 h at 37 $^{\circ}\text{C}$. MBIC was defined as the lowest candesartan cilexetil concentration that resulted in an OD difference at or below 10% of the OD positive control. The MBEC was defined as the lowest concentration that prevents visible growth in the biofilm recovery medium after 18 h incubation.³¹ All assays were repeated in triplicate.

Biolayer Interferometry Assay (BLI). Biotinylated cardiolipin (L-C16B, echelon biosciences, USA) or biotinylated phosphatidylglycerol (L-51B16, echelon biosciences, USA) was employed to determine the binding affinities between candesartan cilexetil and the lipids using a biolayer interferometry assay with Gatorprime (Gator Bio, San Francisco, USA). Streptavidin biosensor tips were utilized for immobilizing the biotin-labeled cardiolipin or phosphatidylglycerol following prewetting with kinetic buffer (PBS, 0.05% bovine serum albumin, 0.01% Tween 20). Subsequently, the

streptavidin biosensors were loaded with varying concentrations of candesartan cilexetil. In order to account for nonspecific and background signals, as well as signal drifts due to biosensor variability, duplicate sets of sensors were utilized as background binding controls and were incubated in buffer without proteins. The assays were performed in 96-well black plates with a total volume of 300 μL /well at 30 $^{\circ}\text{C}$, following a standardized protocol. Data analysis was executed using the Gatorprime data analysis software, applying a double reference subtraction protocol.

Sample Preparation for Quantitative Proteomics Analysis. The clinical *E. faecalis* isolate EF16C166 was cultured overnight and then 1:50 diluted in TSB medium to reach the exponential growth phase ($\text{OD}_{600} \approx 0.5$). Candesartan cilexetil was added to the drug-treated group at a final concentration of 12.5 μM (1/2 \times MIC). The control group was treated with an equal volume of solvent DMSO. Each group was performed with 3 replicates. Following an additional 2 h of incubation at 200 rpm, the bacterial cells were harvested by centrifugation at 4 $^{\circ}\text{C}$ and 5000 rpm for 10 min. The cells were washed twice with precooled PBS and then suspended in RIPA lysis buffer containing 1% Triton X-100, 1% deoxycholate, 0.1% SDS, and complete protease inhibitor cocktail (catalog No. 05892970001, Roche, Basel, Switzerland). The cell suspension was homogenized with glass beads (diameter 0.1 mm) and centrifuged at 12000g for 30 min at 4 $^{\circ}\text{C}$. The resulting supernatant was transferred to new tubes for protein concentration determination and subsequent quantitative proteomics. Protein concentration was determined using the Pierce Micro BCA Protein Assay Kit (catalog No. 23227, Thermo Fisher Scientific, MA, USA). 100 μg of protein was reduced with 10 mM DTT (Sigma-Aldrich Co., St. Louis, MO) for 1 h at 70 $^{\circ}\text{C}$, followed by alkylation with 50 mM iodoacetamide (IAA, Sigma-Aldrich) for 15 min at room temperature in the dark. The samples were desalted three times and buffer-changed with 100 μL of 0.5 M ammonium bicarbonate using Amicon Ultra Centrifugal Filters (10 kDa cutoff; Millipore, Billerica, MA). The proteins were then digested with trypsin at a ratio of 1:50 at 37 $^{\circ}\text{C}$ overnight, lyophilized, and stored at -80°C for mass spectrometry analysis.

Nano LC-MS/MS Analysis for Quantitative Proteomics. The digested protein sample was redissolved in 30 μL of 0.1% formic acid, and 4 μL of the solution was injected into a liquid chromatography (LC) system composed of an UltiMate 3000 RSLC nano system, a C18 precolumn (100 $\mu\text{m} \times 20$ mm, Acclaim PepMap 100 C18, 3 μm), and a C18 tip column (75 $\mu\text{m} \times 250$ mm, Acclaim PepMap RSLC, 2 μm) for separation. The mobile phase consisted of 0.1% formic acid as mobile phase A and 80% acetonitrile with 0.1% formic acid as mobile phase B. The elution system had a flow rate of 300 nL/min, with an initial composition of 5% B for the first 5 min, followed by a linear gradient from 5% to 38% B over the next 85 min, and then from 38% to 95% B for an additional 2 min, maintaining 95% B for 3 more minutes. The LC system was coupled to a Q Exactive Plus mass spectrometer (MS) equipped with a nano spray ionization (NSI) interface. MS1 scans were performed over a mass range of 300–1500 m/z with a resolution of 70,000, while the corresponding MS2 scans had a resolution of 17,500 with a maximum acquisition time of 50 ms. Dynamic exclusion was applied for 30 s to avoid repeated analysis of the same ions, and singly charged

precursor ions and ions of uncertain charge state were excluded from further analysis.

Bioinformatics Analysis for Quantitative Proteomics.

Protein identification and quantification were performed using Proteome Discoverer 2.4 with the Sequest HT, and the analysis was conducted against the Uniprot proteome of *E. faecalis*. Proteins exhibiting a 2-fold cut off value ($p < 0.05$) were considered as upregulated or downregulated. The differentially expressed proteins were then submitted to the OMICSBEAN database (<http://www.omicsbean.com>) for Gene Ontology (GO) annotation, which includes classification into biological processes, cellular components, molecular functions, and KEGG pathway analysis. Additionally, the protein–protein interaction network (PPI network) was analyzed using DAVID.

Statistical Analysis. Graphpad prism 8.0 software was used to process data and draw images. Comparisons of differences in biofilm formation, transcriptional level and CFU between the control group and the sertindole-treated group were analyzed using Student's *t* test. $P < 0.05$ was considered as statistically significant.

■ ASSOCIATED CONTENT

SI Supporting Information

The Supporting Information is available free of charge at <https://pubs.acs.org/doi/10.1021/acsomega.4c02153>.

The MBC distribution of candesartan cilexetil against *E. faecalis* and *E. faecium* (Table S1); MBIC and MBEC of candesartan cilexetil against *E. faecalis* (Table S2) (PDF)

■ AUTHOR INFORMATION

Corresponding Authors

Zhong Chen – Department of Infectious Diseases and Shenzhen Key Laboratory for Endogenous Infections, Huazhong University of Science and Technology Union Shenzhen Hospital, Shenzhen 518052, China; Email: 20024360@163.com

Xiaoju Liu – Department of Infectious Diseases and Shenzhen Key Laboratory for Endogenous Infections, Huazhong University of Science and Technology Union Shenzhen Hospital, Shenzhen 518052, China; Email: 1751566708@qq.com

Authors

Chengchun Chen – Department of Infectious Diseases and Shenzhen Key Laboratory for Endogenous Infections, Huazhong University of Science and Technology Union Shenzhen Hospital, Shenzhen 518052, China; orcid.org/0000-0001-5099-5040

Duoyun Li – Department of Infectious Diseases and Shenzhen Key Laboratory for Endogenous Infections, Huazhong University of Science and Technology Union Shenzhen Hospital, Shenzhen 518052, China

Yongpeng Shang – Department of Infectious Diseases and Shenzhen Key Laboratory for Endogenous Infections, Huazhong University of Science and Technology Union Shenzhen Hospital, Shenzhen 518052, China

Zhiwei Lin – Department of Infectious Diseases and Shenzhen Key Laboratory for Endogenous Infections, Huazhong University of Science and Technology Union Shenzhen Hospital, Shenzhen 518052, China

Zewen Wen – Department of Infectious Diseases and Shenzhen Key Laboratory for Endogenous Infections, Huazhong University of Science and Technology Union Shenzhen Hospital, Shenzhen 518052, China; orcid.org/0000-0002-9934-2056

Peiyu Li – Department of Infectious Diseases and Shenzhen Key Laboratory for Endogenous Infections, Huazhong University of Science and Technology Union Shenzhen Hospital, Shenzhen 518052, China

Zhijian Yu – Department of Infectious Diseases and Shenzhen Key Laboratory for Endogenous Infections, Huazhong University of Science and Technology Union Shenzhen Hospital, Shenzhen 518052, China

Complete contact information is available at:

<https://pubs.acs.org/10.1021/acsomega.4c02153>

Author Contributions

[†]C.C., D.L., Y.S., and Z.L. contributed equally to this work. X.L. and Z.C. conceived and designed the project. C.C., D.L., Y.S., and Z.L. performed the biofilm assay and MIC analysis. Z.W. and P.L. performed the quantitative proteomics experiment. Z.Y. performed the growth curve analysis. All authors participated in data analysis. C.C. and X.L. wrote the manuscript with input from all authors. All authors have read and approved the manuscript. All authors participated in data analysis.

Funding

This work was supported by the following grants: National Nature Science Foundation of China (81902033 and 82002137), Guangdong Basic and Applied Basic Research Foundation (2022A1515110096 and 2021A1515110114), Provincial Medical Funds of Guangdong (A2022497), Shenzhen Key Medical Discipline Construction Fund (SZXK06162), Science, Technology and Innovation Commission of Shenzhen Municipality of Basic Research Funds (JCYJ20190809110209389, JCYJ20190809110622729, JCYJ20220530141614034, and JCYJ20220530141810023), and the Shenzhen Nanshan District Scientific Research Program of the People's Republic of China (2020002, 2020080, NSZD2023019, NS2023049, NS2023097, NS2023027, NS2022026, and YN2022023).

Notes

The authors declare no competing financial interest.

The mass spectrometry proteomics have been deposited to the ProteomeXchange Consortium (<http://proteomecentral.proteomexchange.org>) via the iProX partner repository^{32,33} with the data set identifier PXD044400.

■ REFERENCES

- (1) Fiore, E.; Van Tyne, D.; Gilmore, M. S. Pathogenicity of Enterococci. *Microbiol. Spectrum* **2019**, *7* (4), 10 DOI: [10.1128/microbiolspec.GPP3-0053-2018](https://doi.org/10.1128/microbiolspec.GPP3-0053-2018).
- (2) Lebreton, F.; Manson, A. L.; Saavedra, J. T.; Straub, T. J.; Earl, A. M.; Gilmore, M. S. Tracing the Enterococci from Paleozoic Origins to the Hospital. *Cell* **2017**, *169* (5), 849–861.
- (3) Arias, C. A.; Murray, B. E. The rise of the Enterococcus: beyond vancomycin resistance. *Nat. Rev. Microbiol* **2012**, *10* (4), 266–78.
- (4) Gilmore, M. S.; Salamzade, R.; Selleck, E.; Bryan, N.; Mello, S. S.; Manson, A. L.; Earl, A. M. Genes Contributing to the Unique Biology and Intrinsic Antibiotic Resistance of Enterococcus faecalis. *mBio* **2020**, *11* (6), No. e02962-20, DOI: [10.1128/mBio.02962-20](https://doi.org/10.1128/mBio.02962-20).

- (5) Palmer, K. L.; Kos, V. N.; Gilmore, M. S. Horizontal gene transfer and the genomics of enterococcal antibiotic resistance. *Curr. Opin. Microbiol.* **2010**, *13* (5), 632–9.
- (6) Liu, Y.; Wang, Y.; Schwarz, S.; Li, Y.; Shen, Z.; Zhang, Q.; Wu, C.; Shen, J. Transferable multiresistance plasmids carrying cfr in *Enterococcus* spp. from swine and farm environment. *Antimicrob. Agents Chemother.* **2013**, *57* (1), 42–8.
- (7) Wang, Y.; Lv, Y.; Cai, J.; Schwarz, S.; Cui, L.; Hu, Z.; Zhang, R.; Li, J.; Zhao, Q.; He, T.; Wang, D.; Wang, Z.; Shen, Y.; Li, Y.; Feßler, A. T.; Wu, C.; Yu, H.; Deng, X.; Xia, X.; Shen, J. A novel gene, *optrA*, that confers transferable resistance to oxazolidinones and phenicols and its presence in *Enterococcus faecalis* and *Enterococcus faecium* of human and animal origin. *Journal of antimicrobial chemotherapy* **2015**, *70* (8), 2182–90.
- (8) Chen, L.; Han, D.; Tang, Z.; Hao, J.; Xiong, W.; Zeng, Z. Co-existence of the oxazolidinone resistance genes *cfr* and *optrA* on two transferable multi-resistance plasmids in one *Enterococcus faecalis* isolate from swine. *Int. J. Antimicrob. Agents* **2020**, *56* (1), No. 105993.
- (9) Bi, R.; Qin, T.; Fan, W.; Ma, P.; Gu, B. The emerging problem of linezolid-resistant enterococci. *J. Glob Antimicrob Resist* **2018**, *13*, 11–19.
- (10) Moure, Z.; Lara, N.; Marín, M.; Sola-Campoy, P. J.; Bautista, V.; Gómez-Bertomeu, F.; Gómez-Dominguez, C.; Pérez-Vázquez, M.; Aracil, B.; Campos, J.; Cercenado, E.; Oteo-Iglesias, J. Interregional spread in Spain of linezolid-resistant *Enterococcus* spp. isolates carrying the *optrA* and *poxTA* genes. *Int. J. Antimicrob. Agents* **2020**, *55* (6), No. 105977.
- (11) Joshi, S.; Shallal, A.; Zervos, M. Vancomycin-Resistant Enterococci: Epidemiology, Infection Prevention, and Control. *Infectious disease clinics of North America* **2021**, *35* (4), 953–968.
- (12) Li, W.; Hu, J.; Li, L.; Zhang, M.; Cui, Q.; Ma, Y.; Su, H.; Zhang, X.; Xu, H.; Wang, M. New Mutations in *cls* Lead to Daptomycin Resistance in a Clinical Vancomycin- and Daptomycin-Resistant *Enterococcus faecium* Strain. *Front Microbiol* **2022**, *13*, No. 896916.
- (13) Sandoe, J. A. T.; Witherden, I. R.; Cove, J. H.; Heritage, J.; Wilcox, M. H. Correlation between enterococcal biofilm formation in vitro and medical-device-related infection potential in vivo. *J. Med. Microbiol.* **2003**, *52* (Pt 7), 547–550.
- (14) Zheng, J. X.; Wu, Y.; Lin, Z. W.; Pu, Z. Y.; Yao, W. M.; Chen, Z.; Li, D. Y.; Deng, Q. W.; Qu, D.; Yu, Z. J. Characteristics of and Virulence Factors Associated with Biofilm Formation in Clinical *Enterococcus faecalis* Isolates in China. *Front. Microbiol.* **2017**, *8*, 2338.
- (15) Zheng, J.; Wu, Y.; Lin, Z.; Wang, G.; Jiang, S.; Sun, X.; Tu, H.; Yu, Z.; Qu, D. ClpP participates in stress tolerance, biofilm formation, antimicrobial tolerance, and virulence of *Enterococcus faecalis*. *BMC Microbiol.* **2020**, *20* (1), 30.
- (16) Zheng, J.; Chen, Z.; Lin, Z.; Sun, X.; Bai, B.; Xu, G.; Chen, J.; Yu, Z.; Qu, D. Radezolid Is More Effective Than Linezolid Against Planktonic Cells and Inhibits *Enterococcus faecalis* Biofilm Formation. *Front. Microbiol.* **2020**, *11*, 196.
- (17) Ch'ng, J. H.; Chong, K. K. L.; Lam, L. N.; Wong, J. J.; Kline, K. A. Biofilm-associated infection by enterococci. *Nat. Rev. Microbiol* **2019**, *17* (2), 82–94.
- (18) Balcázar, J. L.; Subirats, J.; Borrego, C. M. The role of biofilms as environmental reservoirs of antibiotic resistance. *Front. Microbiol.* **2015**, *6*, 1216.
- (19) Yan, J.; Bassler, B. L. Surviving as a Community: Antibiotic Tolerance and Persistence in Bacterial Biofilms. *Cell host & microbe* **2019**, *26* (1), 15–21.
- (20) Holmberg, A.; Rasmussen, M. Mature biofilms of *Enterococcus faecalis* and *Enterococcus faecium* are highly resistant to antibiotics. *Diagn Microbiol Infect Dis* **2016**, *84* (1), 19–21.
- (21) Norrby, S. R.; Nord, C. E.; Finch, R. Lack of development of new antimicrobial drugs: a potential serious threat to public health. *Lancet. Infectious diseases* **2005**, *5* (2), 115–9.
- (22) Farha, M. A.; Brown, E. D. Drug repurposing for antimicrobial discovery. *Nature microbiology* **2019**, *4* (4), 565–577.
- (23) Barbee, L. A.; Soge, O. O.; Holmes, K. K.; Golden, M. R. In vitro synergy testing of novel antimicrobial combination therapies against *Neisseria gonorrhoeae*. *J. Antimicrob. Chemother.* **2014**, *69* (6), 1572–8.
- (24) Tran, T. T.; Panesso, D.; Mishra, N. N.; Mileykovskaya, E.; Guan, Z.; Munita, J. M.; Reyes, J.; Diaz, L.; Weinstock, G. M.; Murray, B. E.; Shamoo, Y.; Dowhan, W.; Bayer, A. S.; Arias, C. A. Daptomycin-resistant *Enterococcus faecalis* diverts the antibiotic molecule from the division septum and remodels cell membrane phospholipids. *mBio* **2013**, *4* (4), No. e00281-13, DOI: 10.1128/mBio.00281-13.
- (25) Rashid, R.; Cazenave-Gassiot, A.; Gao, I. H.; Nair, Z. J.; Kumar, J. K.; Gao, L.; Kline, K. A.; Wenk, M. R. Comprehensive analysis of phospholipids and glycolipids in the opportunistic pathogen *Enterococcus faecalis*. *PLoS One* **2017**, *12* (4), No. e0175886.
- (26) Lee, T.; Pang, S.; Abraham, S.; Coombs, G. W. Antimicrobial-resistant CC17 *Enterococcus faecium*: The past, the present and the future. *J. Glob Antimicrob Resist* **2019**, *16*, 36–47.
- (27) Keogh, D.; Tay, W. H.; Ho, Y. Y.; Dale, J. L.; Chen, S.; Umashankar, S.; Williams, R. B. H.; Chen, S. L.; Dunny, G. M.; Kline, K. A. Enterococcal Metabolite Cues Facilitate Interspecies Niche Modulation and Polymicrobial Infection. *Cell host & microbe* **2016**, *20* (4), 493–503.
- (28) Tornero, E.; Senneville, E.; Euba, G.; Petersdorf, S.; Rodríguez-Pardo, D.; Lakatos, B.; Ferrari, M. C.; Pílares, M.; Bahamonde, A.; Trebbe, R.; Benito, N.; Sorli, L.; del Toro, M. D.; Baraiaetxaburu, J. M.; Ramos, A.; Riera, M.; Jover-Sáenz, A.; Palomino, J.; Ariza, J.; Soriano, A. Characteristics of prosthetic joint infections due to *Enterococcus* sp. and predictors of failure: a multi-national study. *Clinical microbiology and infection: the official publication of the European Society of Clinical Microbiology and Infectious Diseases* **2014**, *20* (11), 1219–24.
- (29) Tan, G. S. Q.; Sloan, E. K.; Lambert, P.; Kirkpatrick, C. M. J.; Ilomäki, J. Drug repurposing using real-world data. *Drug discovery today* **2023**, *28* (1), No. 103422.
- (30) Henly, E. L.; Dowling, J. A. R.; Maingay, J. B.; Lacey, M. M.; Smith, T. J.; Forbes, S. Biocide Exposure Induces Changes in Susceptibility, Pathogenicity, and Biofilm Formation in Uropathogenic *Escherichia coli*. *Antimicrob. Agents Chemother.* **2019**, *63* (3), No. e01892-18, DOI: 10.1128/AAC.01892-18.
- (31) Díez-Aguilar, M.; Ekkelenkamp, M.; Morosini, M. I.; Huertas, N.; Del Campo, R.; Zamora, J.; Fluit, A. C.; Tunney, M. M.; Obrecht, D.; Bernardini, F.; Cantón, R. Anti-biofilm activity of murepavidin against cystic fibrosis *Pseudomonas aeruginosa* isolates. *J. Antimicrob. Chemother.* **2021**, *76* (10), 2578–2585.
- (32) Ma, J.; Chen, T.; Wu, S.; Yang, C.; Bai, M.; Shu, K.; Li, K.; Zhang, G.; Jin, Z.; He, F.; Hermjakob, H.; Zhu, Y. iProX: an integrated proteome resource. *Nucleic acids research* **2019**, *47* (D1), D1211–d1217.
- (33) Chen, T.; Ma, J.; Liu, Y.; Chen, Z.; Xiao, N.; Lu, Y.; Fu, Y.; Yang, C.; Li, M.; Wu, S.; Wang, X.; Li, D.; He, F.; Hermjakob, H.; Zhu, Y. iProX in 2021: connecting proteomics data sharing with big data. *Nucleic acids research* **2022**, *50* (D1), D1522–d1527.